CORA Cork Open Research Archive
Cartlann Taighde Oscailte Chorcaí

Title	Microwave assisted low-temperature hydrothermal treatment of solid anaerobic digestate for optimising hydrochar and energy recovery
Authors	Deng, Chen;Kang, Xihui;Lin, Richen;Murphy, Jerry D.
Publication date	2020-04-08
Original Citation	Deng, C., Kang, X., Lin, R. and Murphy, J. D. (2020) 'Microwave assisted low-temperature hydrothermal treatment of solid anaerobic digestate for optimising hydrochar and energy recovery', Chemical Engineering Journal, 395, 124999 (13 pp).
Type of publication	Article (peer-reviewed)
Link to publisher's version	http://www.sciencedirect.com/science/article/pii/S1385894720309918 - 10.1016/j.cej.2020.124999
Rights	© 2020 Elsevier B. V. All rights reserved. This manuscript version is made available under the CC BY-NC-ND 4.0 license. - https://creativecommons.org/licenses/by-nc-nd/4.0/
Download date	2026-10-31 17:46:10
Item downloaded from	https://hdl.handle.net/10468/10202

UCC
University College Cork, Ireland
Coláiste na hOllscoile Corcaigh

*Revised Manuscript (clean for typesetting)
Click here to view linked References

Microwave assisted low-temperature hydrothermal treatment of solid anaerobic digestate for optimising hydrochar and energy recovery

Chen Deng [a, b], Xihui Kang [a, b, c, d], Richen Lin [a, b *], Jerry D Murphy [a, b]

[a] MaREI Centre, Environmental Research Institute, University College Cork, Cork, Ireland

[b] School of Engineering, University College Cork, Cork, Ireland

[c] Guangzhou Institute of Energy Conversion, Chinese Academy of Sciences, Guangzhou, China

[d] University of Chinese Academy of Sciences, Beijing, China

1

[*] Corresponding author:

Dr. Richen Lin, MaREI Centre, Environmental Research Institute, University College Cork, Cork, Ireland. Tel.: +353 (0)21 490 1948. Email: richen.lin@ucc.ie.

Abstract

With the growth of anaerobic digestion (AD) for biogas production, associated increasing digestate production may cause environmental problems if the increasing agricultural land required for digestate application is limited. An alternative is to valorise the digestate. Microwave assisted low-temperature hydrothermal treatment (MLHT; temperature 100–180 °C) was investigated as a post-treatment for AD of grass silage under two scenarios: 1) AD + MLHT and 2) Acid pre-treatment + AD + MLHT. Compared to the original grass silage, the digestates investigated required lower temperatures for carbonization in MLHT owing to their lower cellulose content. The higher MLHT temperatures (160–180 °C) led to significant increases in heating value and greater reductions in atomic ratios of O/C and H/C of hydrochar due to dehydration and decarboxylation reactions. As a result, higher temperatures contributed to higher sugar recovery, higher solid solubilization, and better quality of hydrochar. Under the MLHT at 180 °C, the hydrochar produced from digested grass silage in scenario 1 (AD + MLHT) exhibited a mass yield of 0.79 g/g total solid, a carbon content of 63.6% and an ash-free heating value of 27.6 kJ/g volatile solid; the biomethane potential from the process liquor was estimated as 68.7 ml CH_4/g total solid. Scenario 1 is preferred over scenario 2 (acid pre-treatment + AD + MLHT) as it gave a higher yield and higher heating value of hydrochar. This study suggests that MLHT is a promising method to 1) produce hydrochar with an energy value comparable to lignite coal, and 2) recover additional biomethane through process liquor recycling.

Keywords: Microwave assisted hydrothermal treatment; hydrochar; anaerobic digestion; digestate post-treatment.

1. Introduction

1.1 Environmental challenges associated with anaerobic digestate

Anaerobic digestion (AD) is a proven technology that transforms different organic substrates into biogas and digestate. The ability of AD to digest a multitude of organic substrates ensures its role in waste treatment and renewable energy recovery in "a low carbon, climate-resilient future" [1, 2]. However, AD of feedstock, such as crop straws, agricultural residues and animal slurries, may result in relatively low methane yields due to the recalcitrant structure of the feedstock [3]. A large portion of energy can remain in the anaerobic digestate, mostly associated with the solid fraction of the digestate. Bauer et al determined that approximately 60% of the organic matter in digestate was retrieved in the solid phase after the digestate separation [4].

Traditional application of digestate to agricultural land may not optimise energy return and may in certain cases lead to environmental issues due to strong leachates and associated greenhouse gas emissions. A report from the International Energy Agency Bioenergy highlights that digestate storage and post composting may lead to high levels of methane slippage emissions and negatively affect the overall carbon sustainability of the system [5]. For example, Gioelli et al. calculated the methane emission from non-separated digestate as 1.8 % of the utilized CH_4 [6]. Nicholson et al. reported that NH_3 emission from food-based digestate was 30 – 40% of total nitrogen when applied to agricultural land [7]. Moreover, when the increasing production of digestate exceeds the bearing capacity of local agricultural land, growing demand on the transport and storage of digestate arises, which in turn leads to additional energy consumption and greenhouse gas emissions. This is the primary driver for the development of alternative digestate valorisation routes.

The foregoing suggests the necessity of digestate post-treatment, which if properly managed can minimize methane slippage, reduce non-point source pollution from digestate leachates, reduce fugitive CH_4 emissions, enhance overall carbon sustainability, whilst producing a stable digestion by-product that can be stored and reused.

1.2 Hydrothermal post-treatment of digestate

Hydrothermal treatment can solubilize part of the hemicellulose/lignin fraction, decrease the cellulose crystallinity, and produce high-quality fuels and materials at mild processing conditions [8, 9]. There is no need for a drying treatment of the wet feedstock prior to the hydrothermal process, thus it offers a promising approach for digestate valorisation. The hydrothermal post-treatment of anaerobic digestate at different process temperatures from 160 to 300 °C has been previously investigated with an aim of producing hydrochar as a solid fuel [10]. Funke et al. studied hydrothermal carbonization (HTC) after AD of wheat straw (at 190 to 250 °C) and found that more than half of the energy content in the digestate can be recovered in the hydrochar [11]. Sawatdeenarunat et al. obtained hydrochar with an energy content similar to bituminous coal from digested Napier grass (*Pennisetum purpureum*) at 240 °C [12]. These studies highlighted the feasibility of producing a coal-like biofuel from digestate via hydrothermal post-treatment. Most of these hydrothermal post-treatment processes were conducted at high temperatures or high pressures to ensure highly efficient carbonization of solid digestate [13]; this however required high energy consumption for the process operation and could even lead to a negative energy gain of the process [14]. Despite the progress in hydrochar production from digestate, the investigation on potential for energy and sugar recovery in the hydrothermal process liquor is limited. Nuchdang et al. evaluated the biodegradability of digested microalgae *Scenedesmus* and found that hydrothermal post-treatment at 240 °C and 0.82 MPa enabled a 4-fold improvement in methane yield in subsequent AD of the treated digestate [15]. Unfortunately, no detailed information has been given on the produced hydrochar as a valuable by-product. Aragón-Briceño et al. compared the energy production from sewage sludge under different scenarios, including conventional AD, AD with hydrothermal pre-treatment (HT pre-treatment + AD), and AD with hydrothermal post-treatment (at 160, 220, and 250 °C) followed by a second AD step (AD + HT post-treatment + 2nd AD) [16]. Their results suggested that the HT pre-treatment + AD route presented the highest biomethane production; whilst the route AD + HT post-treatment (at 160 °C) + 2nd AD exhibited lower biomethane yield but higher overall energy production due to the energy recovery in the hydrochar, without consideration of energy consumption for running the processes [16]. Our

previous studies on acid/ hydrothermal pre-treatment also demonstrated the significance of pre-treatment process to enhance biohydrogen and biomethane production from different biomass resources [17, 18]. Inspired by these findings, the combination of pre-treatment, AD, post-treatment, and a second AD may have the potential to increase both the biomethane production and the overall energy production. However, the efficiency of such an integrated scenario depends on multiple process parameters such as the feedstock characteristics, the optimal yield and energy content of various products, the potential impact of up-stream pre-treatment on the post-treatment process, and the energy requirement for running each individual process. As such, the assessment of this integrated scenario has not been well documented in the literature yet.

Microwave irradiation offers a homogenous and faster heating process which can significantly reduce the cost/ time and increase hydrochar yield compared to the conventional hydrothermal process [19]. Previous studies focusing on the microwave assisted hydrothermal pre-treatment of raw biomass have demonstrated its advantages over conventional hydrothermal pre-treatment [20, 21]. Hu et al. found that during the AD of pre-treated cattail the production rate increased by 32% and product yield increased by 19% after microwave pre-treatment at 100 °C, as compared to the conventional water-heating pre-treatment under the same condition [22]. Dai et al. compared microwave assisted and conventional hydrothermal pre-treatment of bamboo sawdust and revealed that the properties of hydrochar from microwave hydrothermal pre-treatment (at 190 and 230°C) were better than those from conventional hydrothermal pre-treatment in terms of calorific value and oxygen content [23]. Microwave assisted hydrothermal process, which has been quite successfully applied in biomass pre-treatment prior to AD, may be a preferable method over conventional hydrothermal treatment for recovering energy and carbonaceous materials from digestate, but the literature is scarce on this topic. The expected benefits of microwave assisted hydrothermal post-treatment approach include for: 1) reducing the greenhouse gas emissions from digestate spreading; 2) improving the overall energy recovery through production of hydrochars and recycling of process liquor for further biomethane production; and 3) saving energy consumed in the process as compared to conventional hydrothermal treatment at higher temperatures. However, the efficiency of such a post-treatment process is

vulnerable to many factors, such as the uncertain hydrochar/ bioenergy potential of different digestates and the potential impact of up-stream pre-treatment process. A gap in the state-of-the-art research is a comprehensive assessment of the efficiency of microwave assisted hydrothermal post-treatment process for digestate valorisation.

1.3 Novelty and objectives

The innovation of this study is to demonstrate a post-treatment process where microwave hydrothermal treatment is applied to digestates from grass silage at a low-temperature range (100–180 °C) for further recovery of hydrochar and biomethane. The detailed objectives are to:

(1) Optimise the yield and qualities of both the hydrochar and the process liquor obtained from microwave assisted low-temperature hydrothermal treatment (MLHT) of digestates;

(2) Compare the carbon/ energy recovery efficiency of two different scenarios, 1) AD + MLHT and 2) Acid pre-treatment + AD + MLHT;

(3) Demonstrate the benefits of the optimised process in terms of the enhancement in biomethane production, hydrochar recovery, and energy efficiency.

2. Materials and methods

2.1 Materials

This study of digestate post-treatment is built upon our previous study of biomethane production from grass silage, in which acid pre-treatment and batch biomethane potential (BMP) assays were investigated [24]. The source of grass silage and the procedure of the BMP assays have been detailed in the previous papers by the authors [24, 25]. Two substrates (untreated grass silage and acid pre-treated grass silage (pre-treated with 2% w/w H_2SO_4 at 135 °C for 15 minutes in an autoclave)) were subjected to the BMP assays. Briefly, the BMP assays were conducted at 35 °C for 30 days in the Bioprocess Control systems (AMPTS II, Sweden) with an inoculum to substrate ratio of 2:1 (measured in volatile solid content). The digestates from both untreated grass silage and pre-treated grass silage were collected after the BMP assays. The digestates (a mix of grass silage residue and

inoculum residue) were centrifuged at 10,000 rpm for 10 min to separate the liquid and solid fractions. The solid fraction, referred to as solid digestate, was oven dried at 80 °C for 72 h and then ground in a ceramic mortar and passed through a 2 mm sieve to ensure a uniform particle diameter and homogenous dry matter content. The prepared samples were refrigerated at 4 °C until further use. Despite the advantage of hydrothermal treatment allowing for the use of wet feedstock, this study dealt with the solid fraction of the digestate, as it contains the majority of the anaerobically nondegraded components which is the major challenge of digestate valorisation [4, 13].

The two distinct digestates and one control group of the original biomass (untreated grass silage) were used as the feedstock for MLHT. These were grouped as follows: *Group 1* solid digestate from untreated grass silage (abbreviated as DU); *Group 2* solid digestate from pre-treated grass silage (abbreviated as DP); and *Group 3* (control group) untreated grass silage (abbreviated as UG). The compositional characteristics of the feedstock are shown in Table 1.

2.2 Microwave assisted low-temperature hydrothermal treatment

The MLHT experiments were conducted in a 2.45 GHz,1600 W microwave oven equipped with Xpress Plus digestion vessels (CEM Mars, UK). In each reaction vessel, 0.7 g of dried feedstock was mixed with 14 ml of distilled water. Then the reaction vessel was sealed and fixed in the microwave oven. The feedstock was heated up to the pre-set temperatures (100, 120, 140, 160, and 180 °C) with a ramp time of 10 minutes and held at the setting temperature for 30 minutes. After the heating process, the reaction vessels were naturally cooled down to room temperature. The solid and liquid products were separated using a centrifuge. The liquid product (namely process liquor) was filtered using a syringe filter with a pore size of 45 μm before compositional analysis. The solid product was oven dried at 80 °C to obtain the hydrochar. The hydrochars were denoted as Char- F-T, where F represents the feedstock (namely UG, DU, and DP) and T represents the MLHT temperature (namely 100, 120, 140, 160, and 180 °C). For example, Char-UG-160 refers to the hydrochar obtained from untreated grass at 160 °C. All experiments were carried out in triplicate. The significance of

differences between means was tested by one-way ANOVA analysis using the software IBM SPSS Statistics v25 with a significance level of $p = 0.05$.

2.3 Biomass and hydrochar characterization methods

To identify the composition of the feedstock and products, the following characterizations were performed. The proximate analysis (analysis of total solid (TS), volatile solid (VS) and ash content) and elemental analysis of the feedstock and hydrochars were conducted according to the methods detailed in a previous paper [24]. The concentration of soluble chemical oxygen demand (sCOD) in the process liquor was determined using the Hach Lange cuvette tests (LCK 914 and LCK 014). To determine the sCOD of the feedstock for the MLHT process, the dried feedstock groups (DU, DP and UG) were each mixed with distilled water at the same liquid-to-solid ratio of 14 ml : 0.7 g. The mixture in the vessel was hand shook, and subsequently left at room temperature for 24 hours before centrifugation to prepare the liquid for sCOD measurement. The reducing sugar content in the process liquor was determined using a High Performance Liquid Chromatography, of which the configuration and method were described in our previous paper [24].

The surface morphology of the hydrochars was obtained on a scanning electron microscope (SEM, Hitachi SU8010, Japan) operated at 200 kV. The specific surface area was measured on a Micrometrics ASAP 2020 analyser and calculated according to the Brunauer-Emmett-Teller (BET) method. The chemical functional groups of the hydrochars were determined using a Fourier transform infrared (FTIR) spectrometer (Nicolet 5700, USA). The crystallinity degree of solid samples was evaluated based on the X-ray diffraction (XRD) patterns in the wide range (5 – 90°) recorded by X'Pert PRO.

2.4 Mass and energy calculation

The product yield of hydrochar was calculated on the basis of TS as follows:

Hydrochar yield = TS in the hydrochar (g) / TS in the feedstock (g) for MLHT (Eq. 1)

The ash-free higher heating value (HHV) of the hydrochar was calculated according to the modified Dulong Formula [26]:

HHV (kJ/kg) = 337C + 1419 (H − 0.125O) + 23.26N (Eq. 2)

in which C, H, O, and N represent the weight percentage of each element in VS.

Energy densification was introduced to indicate the energy retention in hydrochar, which was defined as per Eq. 3:

Energy densification = HHV of hydrochar / HHV of feedstock for MLHT (Eq. 3)

The energy value of the reducing sugars in the process liquor was calculated by the sum of the standard combustion enthalpy of each sugar component (glucose: 2817.3 kJ/mol; xylose: 2342.2 kJ/mol; arabinose: 2336.2 kJ/mol; and cellobiose: 5401.5 kJ/mol [27]).

The energy required for running the MLHT process was calculated based on the following assumptions [14, 28]: 1) the feedstock (a mixture of solid digestate and water) presented the same specific heat capacity and density as water; 2) the environmental temperature was constant at 25 °C; 3) the heat loss during MLHT process was negligible due to the adiabaticity of the reactor. The total energy required for running the MLHT process (Q_{req}) was calculated according to Equation 4.

$$Q_{req} = \rho V_s C(T_p - T_e) \quad \text{(Eq. 4)}$$

in which ρ (1×10^3 kg/m^3) is the density of the feedstock; V_s (m^3) is the volume of the feedstock; C (4.18 kJ/kg/°C) is the specific heat capacity; T_p (°C) is the MLHT temperature; and T_e (°C) is the environmental temperature.

The net energy gain Q_{gain} could be calculated as per Equations 5 and 6.

$$\Delta Q_{CH4} = \Delta H_{CH4} \times (BMP_{post-treated\ D} - BMP_D)/22400 \quad \text{(Eq. 5)}$$

$$Q_{gain} = \Delta Q_{CH4} + Q_{Char} - Q_{req} \quad \text{(Eq. 6)}$$

where ΔQ_{CH4} (kJ/g TS) is the increment of energy content in methane through the MLHT post-treatment of digestate; ΔH_{CH4} is the combustion enthalpy of methane (890.7 kJ/mol); BMP_D (ml/g TS)

and $BMP_{post\text{-}treated\ D}$ (ml/g TS) are the biomethane potential of the original and post-treated digestate samples, respectively; the coefficient (22400) is the unit conversion coefficient from ml/g to mol/g; Q_{char} (kJ/g TS) is the energy content in the produced hydrochar. To compare the net energy gain of MLHT process with the conventional hydrothermal carbonization (HTC), the net energy gain of the HTC post-treatment in the literature was also calculated according to Equations 4 to 6.

3. Results and discussion

3.1 Hydrochar yield, elemental compositions, and energy characteristics

The effects of MLHT temperature on hydrochar yield are presented in Fig. 1. It is clear that higher temperatures led to lower hydrochar yields. As the temperature increased from 100 °C to 140 °C, the hydrochar yield from UG decreased by 2.5% ($p < 0.05$); the hydrochar yield from DU slightly dropped by 1.8% ($p > 0.05$); and the hydrochar yield from DP slightly dropped by 3.5% ($p > 0.05$). When the temperature rose from 140 °C to 180 °C, the hydrochar yields from UG, DU, and DP significantly decreased by 20.2% ($p < 0.05$), 15.1% ($p < 0.05$), and 14.2% ($p < 0.05$), respectively. The hydrochar yields from UG, DU and DP ended up as 0.71, 0.79, and 0.75 g/g TS at 180 °C. The hydrochar yield was slightly lower from the raw biomass UG than that from the digested sample (DU), because most of the degradable fractions (such as hemicellulose and cellulose) were removed from the DU in the up-stream AD process. This was in agreement with a previous study by Zhang et al, in which the hydrochar yield from corn stalk digestate was higher compared to undigested corn stalk at the same condition due to the difference in lignocellulosic components [29].

Table 2 shows the ash content and elemental compositions of the hydrochars produced at different temperatures. The proportional ash content measured in the hydrochars derived from UG ranged between 3.9% and 8.3%; these values slightly decreased as compared to the ash content in UG (10.9%). The MLHT process reduced the ash content as the hydrolysis facilitated solubilization of ash in the aqueous phase. The ash content in the feedstock DU and DP was 31.7% and 35.3%, respectively (Table 1). There is no statistically significant difference ($p > 0.05$) between the ash

content in DU and DP. The ash content in DU derived hydrochars fluctuated between 31.4% and 37.9%. The ash content in DP derived hydrochars fluctuated between 34.4% and 39.4%. The increase in temperature did not result in significant changes in the ash content of hydrochars.

The carbon content in UG derived hydrochars (47.8% – 50.2% of VS) was slightly lower ($p > 0.05$) than the carbon content in UG (50.5% of VS). The oxygen content in the hydrochars derived from UG between 100 °C and 160 °C was higher than that in the original UG (41.3%); the lowest value of 41.2% in UG derived hydrochars was achieved at 180 °C. Two parallel reaction pathways for hydrothermal carbonization of cellulose coexist, which are the "soluble pathway" [30, 31] and the "solid pathway" [32, 33]. The "soluble pathway" takes place in the solution and consists of hydrolysis of cellulose, dehydration of hydrolysis products, and condensation of the soluble species [30, 31]. In the "soluble pathway", the cellulose may lose carbon first due to hydrolysis but will retrieve carbon at a later stage through the condensation of the soluble species. In the "solid pathway", the full cellulose experiences a sequence of reactions including intramolecular condensation, dehydration, and decarboxylation [32, 33]. The cellulose transformed through the "solid pathway" may not experience the loss of carbon at all stages. It is suggested that carbon solubilisation is the predominant pathway at an early reaction stage or under low temperatures and carbon condensation in solid phase occurs after a certain extent of hydrolysis [34, 35]. The insignificant reduction in carbon content in UG derived hydrochars was possibly attributed to the decomposition and solubilisation of the carbohydrates (mainly cellulose and hemicellulose) and crude proteins in UG [36] and limited gas production in the form of H_2, CH_4, and CO_2 [37, 38]. It was accompanied by the formation of reducing sugars in the aqueous phase (as shown in Fig. 4). Similar phenomenon were observed by Su et al. [39] when applying hydrothermal treatment to rice husk at 120 – 150 °C and by Parmar et al. [40] when conducting hydrothermal treatment of digestate from AD of residual municipal solid waste at 150 – 250 °C; however, the variations of carbon content during hydrothermal treatment in their study were feedstock and reaction temperature dependent.

The carbon content in the hydrochars derived from DU and DP showed a decreasing – increasing trend as the temperature increased from 100 °C to 180 °C. This variation trend of carbon content was in accordance with the reaction mechanism of cellulose – coexistence of two parallel reaction pathways, namely "soluble pathway" and "solid pathway". The carbon content in hydrochars derived from DU and DP was higher compared to the feedstock DU and DP. As the temperature reached 180 °C, the carbon content in DU derived hydrochar achieved 63.6%, significantly higher ($p < 0.05$) than 54.4% in DU; the carbon content in DP derived hydrochar achieved 60.2%, significantly higher ($p < 0.05$) than 55.5% in DP. The oxygen content in the digestates derived hydrochars decreased compared to that in the digestates feedstock. The initial oxygen content in DU and DP was 33.3% and 33.0% on a VS basis, respectively. After MLHT at 180 °C, the oxygen content in the hydrochars derived from DU and DP decreased to 24.5% and 28.8%, respectively. In addition, the hydrogen content in the hydrochars derived from DU and DP increased to 7.3% and 6.9% at 180 °C, respectively. The increased carbon content and decreased oxygen content in these hydrochars implied the carbonization of DU and DP in MLHT process.

To further understand the change of elemental composition, the atomic ratios of hydrogen to carbon (H/C) and oxygen to carbon (O/C) in both the feedstock and the derived hydrochars were plotted in a van-Krevelen diagram displayed in Fig. 2. The van-Krevelen space was divided into several regions by the dash lines; the stoichiometric ranges were used to establish boundaries of the classification space for cellulose, amino sugars, proteins, lignin, peat, and lignite [41, 42]. Trends along the arrows reflect reaction pathways by indicating the change of elements in a specific molar ratio [43, 44]. The elemental composition of the feedstock UG fell into the amino sugar region, which is a transition section between cellulose, lignin and protein regions. The elemental compositions of DU and DP fell into the regions close to the junction of proteins and lignin as most of the cellulose and hemicellulose were degraded in the AD process. At lower temperatures, a decrease in H/C and an increase in O/C among the three types of hydrochars suggested that the demethylation hydrolysis reactions were in dominance [42, 45]. Zhang et al. reported that the barely observed change of carbon content indicated that hydrolysis was the main reaction path during solubilisation of cellulose at low temperature [34].

When the temperature increased from 160 to 180 °C, hydrochars showed great reductions in both O/C and H/C leading to the increase of proportional carbon content, which was considered as the major indicator of condensation reactions such as dehydration and decarboxylation reactions [35, 45, 46]. The elemental composition of all the hydrochars obtained at 180 °C fell into the region represented by lignin. The hydrochars derived from DU and DP at 180 °C became close to lignite in terms of the atomic H/C and O/C ratios. Under MLHT at 180 °C, the UG derived hydrochar presented an atomic O/C ratio of 0.62, similar to the ratio of 0.61 in UG ($p > 0.05$); the DU derived hydrochar presented a significantly reduced atomic O/C ratio of 0.29 compared to the ratio of 0.46 in DU ($p < 0.05$); the DP derived hydrochar presented a significantly reduced atomic O/C ratio of 0.36 compared to the ratio of 0.45 in DP ($p < 0.05$). The atomic O/C ratio is an index of the carbonization degree and the stability of the hydrochar. It indicated that a greater degree of carbonization occurred in the MLHT post-treatment of digestates compared to the raw biomass. This may be due to the difference in components between the digestates and untreated grass silage, as cellulose, lignin, and other hydrocarbons react at different temperatures [47]. Mumme et al. [48] observed that digested maize silage was hydrothermally carbonized at 190 °C but pure cellulose did not show signs of carbonization at the same temperature; their explanation was that the presence of hydrogen bonds in cellulose increased the temperature required for carbonization above those required for glucose, starch, and sucrose. Zhai et al. observed that the carbonization of pure cellulose took place at temperatures exceeding 210 °C [49]. It could be inferred that the higher cellulose content in the untreated grass silage led to a higher temperature required for carbonization, that is a lower carbonization reactivity compared to the digested grass silage. In addition, the complexity of the digestate due to its high ash content may induce a catalytic effect on the carbonization under mild thermal conditions [50]. Further investigations are needed to reveal the effect of mineral compounds.

The ash-free HHV of the hydrochars produced at different temperatures are presented in Fig. 3. Many authors have reported an increased HHV of hydrochars compared to the initial substrates [20, 42]. In this study, the HHVs of the UG derived hydrochars were significantly lower ($p < 0.05$) than the HHV of original UG due to the solubilisation of carbohydrates. The hydrochar derived from UG at 180 °C

presented an HHV of 18.4 kJ/g VS, significantly lower ($p < 0.05$) than 19.0 kJ/g VS of the feedstock UG. Its ash content of 4.2% generates an energy value on a dry mass basis (allowing for ash content) of 17.6 kJ/kg TS. As the O/C ratio and energy retention in the hydrochar act as two major quantitative indexes for carbonization degree [34], the lower carbon content and lower HHV of the UG derived hydrochars compared to UG may suggest that no carbonization but only solubilisation occurred during the MLHT treatment of UG. In contrast, the hydrochars derived from DU and DP had higher HHVs than their corresponding feedstock DU and DP. As the temperature rose from 160 °C to 180 °C, a significant increase ($p < 0.05$) in the HHV was observed for both DU and DP derived hydrochars; this was also evident for the occurrence of carbonization. Similarly, Knappe et al. reported that the major increase in the heating value of hydrochar derived from willow took place at 170 °C [51]. At 180 °C, the DU derived hydrochar presented a significantly higher ($p < 0.05$) HHV of 27.6 kJ/g VS compared to 22.3 kJ/g VS of DU; the DP derived hydrochar presented a significantly higher ($p < 0.05$) HHV of 25.1 kJ/g VS compared to 22.4 kJ/g VS of DP. Calculated on a dry mass basis (allowing for ash content), the energy value of the DU derived hydrochar at 180 °C achieved 17.1 kJ/g TS, which is comparable to those of lignite coal (15 – 20 kJ/g) [52] and sub-bituminous coal (21 kJ/g) [12]. However, the hydrochars derived from DU and DP at 180 °C contained 37.9% and 39.4% ash, as such they would not be classified as a high-quality fuel.

3.2 Reducing sugar and sCOD yields in the process liquor

The composition of monosaccharides and disaccharides in the process liquor are shown in Fig. 4. During the MLHT of UG, cellobiose and glucose were released due to the hydrolysis of cellulose; xylose and arabinose were released due to the hydrolysis of hemicellulose [53]. With increasing temperature, the yield of reducing sugars from UG peaked at 140 °C, giving a maximum value of 15.2 mg/g TS (Fig. 4 a). Further increasing the temperature beyond 140 °C decreased sugar recovery due to the denaturation of sugars. The reducing sugar yields from DU and DP were much lower compared to those from UG. An explanation is that the readily available carbohydrates have been digested during the AD process leaving a digestate with higher lignin and ash contents than the original biomass. Therefore, a relatively small portion of digestates was degraded during the MLHT process,

leading to lower reducing sugar yields from DU and DP. The reducing sugar yields from both DU and DP increased with the increased temperature. The maximum reducing sugar yields from DU and DP were 6.5 and 4.5 mg/g TS obtained at 180 °C (Fig. 4 b and c).

The initial sCOD value of the untreated grass silage was measured as 155 mg/g TS, while the initial sCOD values of DU and DP were both less than 20 mg/g TS (data not shown). The sCOD values in the process liquor derived at different temperatures are shown in Fig. 5. The solubilisation of the feedstock increased with the increase in temperature. Although the three substrates had different initial sCOD values, the process liquor produced at 180 °C showed a similar maximum sCOD value of ca. 200 mg/g TS. The increase in sCOD was much higher than the increase in reducing sugars during the MLHT of digestates DU and DP. The difference between the concentration of reducing sugars and that of sCOD may be attributed to the formation of lignin and protein derivatives. Correa et al. observed the generation of small molecules such as syringol, ethylguaiacol, and guaiacol from lignin decomposition through hydrolysis reactions and cleavage of ether bonds, which were dominant reactions at temperatures below 200 °C [50]. The sCOD may be a potential substrate for further biomethane production through AD. The theoretical biomethane yield is reported to be approximately 350 ml CH_4/g sCOD from wastewater [54, 55]. Based on this the maximum biomethane potential of the process liquor derived at 180 °C was estimated as 72.8, 68.7, and 72.7 ml from per gram UG, DU and DP (TS basis), respectively. The recycling of process liquor in HTC has also been reported to enhance the yield and heating value of the produced hydrochar due to the increase in the acidity of the process liquor from recycling, which facilitates the decarboxylation and dehydration reactions [56]. This may offer another opportunity for the use of process liquor.

3.3 Energy and carbon distribution in the products

The energy distribution in each product from the MLHT can be determined based on the HHV of hydrochar and the energy content of reducing sugars in the process liquor. The results are displayed in Fig. 6. Among the products obtained from the substrates, the hydrochars accounted for the majority of the energy, ranging from 73.8% to almost 100% of the total energy contained in the products. For the

products derived from UG, reducing sugars in the process liquor produced at 140 °C contained 1.4% of the energy content in the products, which was the highest share of energy in the reducing sugars as compared to those obtained under other temperatures. For the products from DU and DP, the highest share of energy in the reducing sugars was only 0.6% and 0.5%, respectively.

Fig.7. shows the carbon distribution in the entire processes under the two different scenarios, namely 1) AD + MLHT and 2) Acid pre-treatment + AD + MLHT. The entire processes were evaluated from raw grass silage to the end products, including for biomethane, carbon dioxide, liquid digestate, process liquor from MLHT, and hydrochar. The data of biogas and digestate production was obtained from previous work by the authors [24]. In the case study of both scenarios, the acid pre-treatment was conducted with 2% w/w sulphuric acid at 135°C for 15 minutes and the MLHT of the digestates was conducted at 180°C. In the first scenario of AD + MLHT, as shown in Fig.7 a, 45.9% of the carbon from grass silage flowed into biogas (CH_4 + CO_2), 46.3% of the carbon remained in the hydrochar; the rest of the carbon remained in the liquid digestate of AD and the process liquor/ gases produced in the MLHT. In the second scenario of acid pre-treatment + AD + MLHT, as shown in Fig.7 b, 41.7% of the carbon from grass silage flowed into biogas, and 44.1% of the carbon remained in the hydrochar. In the second scenario with pre-treatment prior to AD, less carbon flowed into gaseous products caused by the possible sodium inhibition in the AD process; less carbon remained in the hydrochar. The loss of carbon in the detected products resulted in an uncertainty of the fate of carbon. In contrast to the traditional linear biogas supply chain of “biomass pre-treatment, biogas production, digestate application to agricultural land”, the MLHT post-treatment extended the utilisation of biomass resources by reusing digestate for hydrochar production and recycling process liquor. The concentration of carbon in the hydrochar with further application makes the entire supply chain more carbon sustainable within the concept of zero-waste circular bioeconomy. The properties of the produced hydrochars must be identified before its proper application route can be determined.

3.4 Properties of the hydrochar

The SEM images in Fig. 8 illustrate the morphological variations between the feedstock and the derived hydrochars. The surface of the untreated grass silage was smooth and compact as shown in Fig. 8 (a). The development of pores and cracks were observed on the surface of solid digestates DU and DP (as shown in Fig. 8 (c) and (e)) caused by the degradation of cellulose and hemicellulose in the AD process. After the MLHT process, UG derived hydrochar showed an uneven surface and hydrochars from DU and DP presented much rougher and porous surfaces. The BET results indicated an increase in the specific surface area of all the hydrochars compared to their corresponding feedstock. The specific surface areas of UG, DU and DP were 1.7, 3.1, and 3.8 m^2/g, respectively. Under the MLHT at 160 °C, the UG derived hydrochar presented a low specific surface area of 2.8 m^2/g; the DU and DP derived hydrochars presented specific surface areas of 7.5 and 7.7 m^2/g, respectively, which were consistent with what was expected from the literature [48, 50]. The hydrochars produced from the model substrates of lignin (at 300 °C), cellulose (at 300 °C), and hemicellulose (at 250 °C) were reported to exhibit specific surface areas of 2.3, 13.2, and 9.3 m^2/g, respectively [57].

The XRD pattern shown in Fig. 9 was used to determine the changes in the crystallinity of the substrates and the hydrochars. The wide intensity peaks centred at 15.9° and 21.7° for untreated grass silage were attributed to the presence of cellulose with crystalline structure [58], both of which disappeared in the digestates (DU and DP) due to the degradation in the AD. The crystalline structure of cellulose remained in the hydrochar derived from UG owing to the strong thermal stability of cellulose. Compared to the feedstock DU and DP, no obvious changes were observed in the XRD patterns of the corresponding hydrochars. There were some sharp peaks in the patterns of digestates and digestates derived hydrochars, which could be ascribed to inorganic crystals carried over by the inoculum such as $Ca_3(PO_4)_2$, $Mg_3(PO4)_2$, or $CaCO_3$ [59].

The substrates and derived hydrochars were characterized by infrared spectroscopy as shown in Fig. 10. All hydrochars showed similar peaks to their corresponding feedstock, which was due to the fact

that the process temperature was not high enough to result in significant changes in major functional groups. Differences existed between the hydrochar derived from untreated grass silage and the hydrochars from the digestates. The absorbance peak at 2926 cm^{-1}, which represents the aliphatic C–H stretch vibration [57], stood out in the spectra of the digestates and digestates derived hydrochars, showing an increased degree of condensation and aromaticity. The peak at 1650 cm^{-1} which is associated with aromatic C=C presented a slight enhancement in the spectra of the digestates and digestates derived hydrochars, suggesting the structure of lignin was relatively stable [60].

3.5 Energetic potential

The development of efficient and profitable routes for digestate valorisation has drawn increasing research interest. A few studies have investigated the residual methane potential of anaerobic digestate, but the results vary depending on the properties of digestate and the post-treatment methods [13]. For example, Ruile et al. obtained values of residual methane potential ranging from 24 to 126 ml CH_4 /g VS when evaluating digestates from mesophilic full-scale anaerobic digesters fed with manure and energy crops [61]. If this residual methane potential is realised and is released in open storage systems for digestate, it reduces the GHG sustainability of the overall system (Global Warming Potential of CH_4 = 28) possibly to the extent that the biogas produced may not meet sustainable requirements as defined by the recast Renewable Energy Directive (2018/2001/EU) [62]. Some researchers have investigated the application of post-treatment to enhance the methane production (and collection) from digestates. In a study conducted by Sambusiti et al., the methane potential of the raw solid digestate (sourced from a mesophilic AD plant processing mixed maize silage, sorghum silage, olive waste, cow manure, pig manure, and turkey poultry manure) was 90 ml/g VS; this value increased to 102 ml/g VS after enzymatic treatment of the digestate but did not increase after thermal (at 80 °C) or alkaline treatment of the digestate [63]. In contrast mild thermal post-treatment at a higher temperature (120 °C for 30 min) enhanced the methane potential of solid digestates from two different AD plants by 12 – 115% [64]. In this study, the methane recovery potentials from the MLHT process liquor obtained at 180 °C were 68.7 ml/g TS of DU and 72.7 ml/g TS of DP (equivalent to 110.7 ml/g VS of DU and 119.8 ml/g VS of DP), respectively, which were

comparable to the methane potentials from digestates reported in the above cited literature. The recirculation of process liquor can enhance the overall energy conversion of the original feedstock, decrease the volume of the recirculated digestate, and reduce the greenhouse gas emissions from the digestate storage/ transport, thereby contributing to reducing the environmental impact of digestate disposal.

Owing to the destruction of the lignocellulosic matrix in AD, the derived solid digestate was favourable for carbonization in MLHT process over the raw biomass as evidenced by the Van-Krevelen diagram (Fig. 2). The hydrochars generated from the digestate have been reported to exhibit heating values comparable to those of coals [29]. Table 3 compares the energy content of hydrochars obtained through MLHT of digestates in this study and hydrochars obtained through HTC of diverse digestates under similar conditions in the literature. In this study, even at a relatively low hydrothermal temperature of 180 °C, the hydrochars derived from DU and DP present ash free HHVs of 27.6 and 25.1 kJ/g VS, respectively. The energy value of hydrochar is feedstock and process condition dependent. As such it is meaningless to compare the HHV of diverse hydrochars directly. Energy densification is used to indicate the energy retention in different processes. The energy densification values reached 1.24 and 1.12 for DU and DP derived hydrochars, respectively, which were higher than most of those obtained from HTC of digestates listed in Table 3. Mumme et al. obtained a higher energy densification of 1.36 at a much higher temperature of 230 °C with longer reaction time [48]. Sharma et al obtained higher energy densifications of 1.31 and 1.37 at 180 °C and 200 °C when the reaction time was significantly extended to 360 min [65]. From the perspective of energy densification, MLHT of digestate enables higher energy retention in hydrochars compared to conventional HTC as microwave heating allows for faster and more uniform heat transfer. However, the high ash content in the digestate, which may cause problems such as slagging, fouling, and corrosion in the combustion units, is the main obstacle to the combustion of the derived hydrochars. To improve the carbon content and thermal stability of hydrochars requires increased treatment temperature, which on the other hand may lower the net energy gain due to the increased energy consumption associated with the process operation [66]. The increased operational costs such as

hydrothermal post-treatment of digestate, circulation of process liquor, and pelletisation of hydrochar must be compensated by the increment in energy and environment gains for engineering implications.

Table 4 shows the comparison of net energy gain from post-treatment of anaerobic digestate through MLHT in this study and conventional HTC in the literature. Under Scenario 1, the MLHT of DU at 180 °C led to an energy increment in methane of 2.5 kJ/g TS of DU and an energy content of 13.5 kJ/g TS of DU in the derived hydrochar. Considering that the energy required for treating 1 g TS of DU was 13.6 kJ, the net energy gain was 2.4 kJ/g TS of DU under this scenario. Under Scenario 2, the net energy gain from the MLHT of DP at 180 °C was 0.4 kJ/g TS of DP. The lower net energy gain under Scenario 2 was ascribed to the lower energy content in the hydrochar compared to Scenario 1. The studies by Yuan et al. [14] and Aragón [16] have shown that HTC temperature is an important factor affecting the net energy gain from the post-treatment. The HTC of digested sewage sludge at 160 °C led to a positive net energy gain (1.9 kJ/g TS of solid digestate); when the HTC temperature increased to 220 °C, the net energy gain reduced to a negative value (–4.7 kJ/g solid digestate) even with a 7% increase in methane potential from the process liquor, due to a 45% increase in energy requirement for running the process [16]. The HTC of digested microalgae at 200 °C resulted in a 141% increment of energy in methane, which was still insufficient to cover the energy required for running the process [15]. Another key factor affecting the net energy gain is the solid loading in the digestate feedstock. A high solid loading can significantly increase the net energy gain by reducing the energy required for running the process. The HTC of solid digestate from Napier grass (*Pennisetum purpureum*) at 240 °C resulted in a positive net energy gain of 5.2 kJ/g TS of solid digestate due to a high solid concentration of 14.3% in the digestate feedstock [12]. This implies that for large-sale applications a high solid content could be used to improve the energy gain of post-treatment. The present energy calculation was based on a batch scale investigation, where 2 g VS of substrate was tested in each AD reactor. The small scale of sampling may lead to a limitation in quantifying the mass/ energy balance. However, these batch tests can serve as a design of larger scale continuous digesters providing a bigger source of samples to validate the applicability of digestate post-treatment at a commercial scale.

In summary, MLHT of solid digestate into energy or value-added products is promising as an extension to traditional farmland application. Process liquor of the MLHT may be recirculated back to the digester to allow for more efficient organic matter removal and higher methane yield. There are many applications of hydrochars including but not limited to energy production, carbon sequestration, agriculture, and wastewater treatment [67, 68]. Similar to biochar, the hydrochar amended into fields may act as a carbon sink by stimulating microbial CH_4 respiration or microbial metabolism of CH_4 [69, 70]. The global negative emission potential of the addition of biochar to land could be up to 0.7 Gt C/year based on an assumed application rate of 50 t/ha and a land footprint of 14 Mha [71]. In a world where the threat of climate change is deemed an emergency, the use of hydrochar as a means of increasing soil organic content may be deemed pragmatic.

4. Conclusions

Microwave assisted low-temperature hydrothermal treatment (MLHT) of solid digestates was demonstrated as an effective post-treatment process for anaerobic digestion (AD) to improve energy and carbon recovery. As compared to hydrochar derived from the original grass silage, the hydrochars from the digested grass silage exhibited clear advantages, including higher mass yield and higher heating value per gram VS (on an ash free basis). MLHT at 180 °C was assessed as the most beneficial for carbon and energy recovery from the digestates. In scenario 1) AD + MLHT at 180 °C: hydrochar produced from digestated grass silage exhibited a mass yield of 0.79 g/g TS, a carbon content of 63.6%, and an ash-free heating value of 27.6 kJ/g VS; the biomethane potential of the process liquor was estimated as 68.7 ml/g TS of digested grass silage. The scenario 2) acid pre-treatment + AD + MLHT gave a lower yield and lower heating value of hydrochars but a slightly higher methane potential from the process liquor. Further research to implement the pilot scale experiments is required to ensure the techno-economic feasibility of the entire technological route.

Acknowledgements

This study was funded by Science Foundation Ireland (SFI) through the MaREI Centre for energy, climate and marine under Grant No. 12/RC/2302 and 16/SP/3829 and by European Regional Development Fund under the Interreg NWE Project (NWE 964). This work was also supported by the European Union's Horizon 2020 research and innovation program under the Marie Skłodowska-Curie grant (No. 797259) and the Environmental Protection Agency – Ireland (2018-RE-MS-13). Industrial co-funding from Gas Networks Ireland through the Gas Innovation Group is also gratefully acknowledged.

References

[1] A. Raheem, V.S. Sikarwar, J. He, W. Dastyar, D.D. Dionysiou, W. Wang, M. Zhao, Opportunities and challenges in sustainable treatment and resource reuse of sewage sludge: A review, Chem. Eng. J. 337 (2018) 616-641.

[2] P.G. Kougias, I. Angelidaki, Biogas and its opportunities—A review, Front. Env. Sci. Eng. 12 (2018) 14.

[3] A. Cesaro, V. Belgiorno, Pretreatment methods to improve anaerobic biodegradability of organic municipal solid waste fractions, Chem. Eng. J. 240 (2014) 24-37.

[4] A. Bauer, H. Mayr, K. Hopfner-Sixt, T. Amon, Detailed monitoring of two biogas plants and mechanical solid-liquid separation of fermentation residues, J. Biotechnol. 142 (2009) 56-63.

[5] T.R. Jan Liebetrau, Alessandro Agostini, Bernd Linke, Methane emissions from biogas plants, IEA Bioenergy: Task 37 12 (2017) 1-52.

[6] F. Gioelli, E. Dinuccio, P. Balsari, Residual biogas potential from the storage tanks of non-separated digestate and digested liquid fraction, Bioresour. Technol. 102 (2011) 10248-10251.

[7] F. Nicholson, A. Bhogal, L. Cardenas, D. Chadwick, T. Misselbrook, A. Rollett, M. Taylor, R. Thorman, J. Williams, Nitrogen losses to the environment following food-based digestate and compost applications to agricultural land, Environ. Pollut. 228 (2017) 504-516.

[8] L. Baskoro, A. Muhammad, K. Yoshikawa, F. Takahashi, Energy and resource recovery from Tetra Pak waste using hydrothermal treatment, Appl. Energy 207 (2017) 107-113.
[9] A. Jain, R. Balasubramanian, M.P. Srinivasan, Hydrothermal conversion of biomass waste to activated carbon with high porosity: A review, Chem. Eng. J. 283 (2016) 789-805.
[10] M. Pecchi, M. Baratieri, Coupling anaerobic digestion with gasification, pyrolysis or hydrothermal carbonization: A review, Renew. Sustain. Energy. Rev. 105 (2019) 462-475.
[11] A. Funke, J. Mumme, M. Koon, M. Diakité, Cascaded production of biogas and hydrochar from wheat straw: Energetic potential and recovery of carbon and plant nutrients, Biomass Bioenerg. 58 (2013) 229-237.
[12] C. Sawatdeenarunat, H. Nam, S. Adhikari, S. Sung, S.K. Khanal, Decentralized biorefinery for lignocellulosic biomass: Integrating anaerobic digestion with thermochemical conversion, Bioresour. Technol. 250 (2018) 140-147.
[13] F. Monlau, C. Sambusiti, E. Ficara, A. Aboulkas, A. Barakat, H. Carrère, New opportunities for agricultural digestate valorization: current situation and perspectives, Energy Environ. Sci. 8 (2015) 2600-2621.
[14] T. Yuan, Y. Cheng, Z. Zhang, Z. Lei, K. Shimizu, Comparative study on hydrothermal treatment as pre- and post-treatment of anaerobic digestion of primary sludge: Focus on energy balance, resources transformation and sludge dewaterability, Appl. Energy 239 (2019) 171-180.
[15] S. Nuchdang, J.C. Frigon, C. Roy, G. Pilon, C. Phalakornkule, S.R. Guiot, Hydrothermal post-treatment of digestate to maximize the methane yield from the anaerobic digestion of microalgae, Waste Manag. 71 (2018) 683-688.
[16] C. Aragón-Briceño, A.B. Ross, M.A. Camargo-Valero, Evaluation and comparison of product yields and bio-methane potential in sewage digestate following hydrothermal treatment, Appl. Energy 208 (2017) 1357-1369.
[17] R. Lin, C. Deng, L. Ding, A. Bose, J.D. Murphy, Improving gaseous biofuel production from seaweed Saccharina latissima The effect of hydrothermal pretreatment on energy efficiency, Energy Convers. Manage. 196 (2019) 1385-1394.

[18] C.H. Sun, A. Xia, Q. Fu, Y. Huang, R.C. Lin, J.D. Murphy, Effects of pre-treatment and biological acidification on fermentative hydrogen and methane co-production, Energy Convers. Manage. 185 (2019) 431-441.

[19] A. Aguilar-Reynosa, A. Romani, R.M. Rodriguez-Jasso, C.N. Aguilar, G. Garrote, H.A. Ruiz, Comparison of microwave and conduction-convection heating autohydrolysis pretreatment for bioethanol production, Bioresour. Technol. 243 (2017) 273-283.

[20] L. Cao, I.K.M. Yu, D.W. Cho, D. Wang, D.C.W. Tsang, S. Zhang, S. Ding, L. Wang, Y.S. Ok, Microwave-assisted low-temperature hydrothermal treatment of red seaweed (Gracilaria lemaneiformis) for production of levulinic acid and algae hydrochar, Bioresour. Technol. 273 (2019) 251-258.

[21] O.O.D. Afolabi, M. Sohail, C.L.P. Thomas, Characterization of solid fuel chars recovered from microwave hydrothermal carbonization of human biowaste, Energy 134 (2017) 74-89.

[22] Z.-H. Hu, Z.-B. Yue, H.-Q. Yu, S.-Y. Liu, H. Harada, Y.-Y. Li, Mechanisms of microwave irradiation pretreatment for enhancing anaerobic digestion of cattail by rumen microorganisms, Appl. Energy 93 (2012) 229-236.

[23] L. Dai, C. He, Y. Wang, Y. Liu, Z. Yu, Y. Zhou, L. Fan, D. Duan, R. Ruan, Comparative study on microwave and conventional hydrothermal pretreatment of bamboo sawdust: Hydrochar properties and its pyrolysis behaviors, Energy Convers. Manage. 146 (2017) 1-7.

[24] C. Deng, R. Lin, J. Cheng, J.D. Murphy, Can acid pre-treatment enhance biohydrogen and biomethane production from grass silage in single-stage and two-stage fermentation processes?, Energy Convers. Manage. 195 (2019) 738-747.

[25] R. Lin, J. Cheng, L. Ding, J.D. Murphy, Improved efficiency of anaerobic digestion through direct interspecies electron transfer at mesophilic and thermophilic temperature ranges, Chem. Eng. J. 350 (2018) 681-691.

[26] A.S. Nizami, Korres, N E. , Murphy, J D., Review of the Integrated Process for the Production of Grass Biomethane, Environ. Sci. Technol. 43 (2009) 8496-8508.

[27] NIST Chemistry WebBook. , National Institute of Standards and Technology, Available on: https://webbook.nist.gov/chemistry/.

[28] W. Huang, Z. Zhao, T. Yuan, W. Huang, Z. Lei, Z. Zhang, Low-temperature hydrothermal pretreatment followed by dry anaerobic digestion: A sustainable strategy for manure waste management regarding energy recovery and nutrients availability, Waste Manag. 70 (2017) 255-262.
[29] D. Zhang, F. Wang, X. Shen, W. Yi, Z. Li, Y. Li, C. Tian, Comparison study on fuel properties of hydrochars produced from corn stalk and corn stalk digestate, Energy 165 (2018) 527-536.
[30] Y. Ogihara, R.L. Smith, H. Inomata, K. Arai, Direct observation of cellulose dissolution in subcritical and supercritical water over a wide range of water densities (550–1000 kg/m3), Cellulose 12 (2005) 595-606.
[31] M. Sevilla, A.B. Fuertes, The production of carbon materials by hydrothermal carbonization of cellulose, Carbon 47 (2009) 2281-2289.
[32] C. Falco, N. Baccile, M.-M. Titirici, Morphological and structural differences between glucose, cellulose and lignocellulosic biomass derived hydrothermal carbons, Green Chem. 13 (2011).
[33] B. Hu, K. Wang, L. Wu, S.H. Yu, M. Antonietti, M.M. Titirici, Engineering carbon materials from the hydrothermal carbonization process of biomass, Adv. Mater. 22 (2010) 813-828.
[34] J. Zhang, Y. An, A. Borrion, W. He, N. Wang, Y. Chen, G. Li, Process characteristics for microwave assisted hydrothermal carbonization of cellulose, Bioresour. Technol. 259 (2018) 91-98.
[35] E. García-Bordejé, E. Pires, J.M. Fraile, Parametric study of the hydrothermal carbonization of cellulose and effect of acidic conditions, Carbon 123 (2017) 421-432.
[36] X. Kang, Y. Sun, L. Li, X. Kong, Z. Yuan, Improving methane production from anaerobic digestion of Pennisetum Hybrid by alkaline pretreatment, Bioresour. Technol. 255 (2018) 205-212.
[37] J. Poerschmann, I. Baskyr, B. Weiner, R. Koehler, H. Wedwitschka, F.D. Kopinke, Hydrothermal carbonization of olive mill wastewater, Bioresour. Technol. 133 (2013) 581-588.
[38] X. Xu, E. Jiang, Treatment of urban sludge by hydrothermal carbonization, Bioresour. Technol. 238 (2017) 182-187.
[39] Y. Su, L. Liu, D. Xu, H. Du, Y. Xie, Y. Xiong, S. Zhang, Syngas production at low temperature via the combination of hydrothermal pretreatment and activated carbon catalyst along with value-added utilization of tar and bio-char, Energy Convers. Manage. 205 (2020).

[40] K.R. Parmar, A.B. Ross, Integration of Hydrothermal Carbonisation with Anaerobic Digestion; Opportunities for Valorisation of Digestate, Energies 12 (2019).

[41] T. Ohno, Z. He, R.L. Sleighter, C.W. Honeycutt, P.G. Hatcher, Ultrahigh resolution mass spectrometry and indicator species analysis to identify marker components of soil-and plant biomass-derived organic matter fractions, Environ. Sci. Technol. 44 (2010) 8594-8600.

[42] R.K. Garlapalli, B. Wirth, M.T. Reza, Pyrolysis of hydrochar from digestate: Effect of hydrothermal carbonization and pyrolysis temperatures on pyrochar formation, Bioresour. Technol. 220 (2016) 168-174.

[43] R.L. Sleighter, P.G. Hatcher, The application of electrospray ionization coupled to ultrahigh resolution mass spectrometry for the molecular characterization of natural organic matter, J. Mass Spectrom. 42 (2007) 559-574.

[44] R.W.K. Sunghwan Kim, Patrick G. Hatcher, Graphical Method for Analysis of Ultrahigh-Resolution Broadband Mass Spectra of Natural Organic Matter, the Van Krevelen Diagram, Anal. Chem. 75 (2003) 5336-5344.

[45] K.Y. Park, K. Lee, D. Kim, Characterized hydrochar of algal biomass for producing solid fuel through hydrothermal carbonization, Bioresour. Technol. 258 (2018) 119-124.

[46] Y. Zhang, Q. Jiang, W. Xie, Y. Wang, J. Kang, Effects of temperature, time and acidity of hydrothermal carbonization on the hydrochar properties and nitrogen recovery from corn stover, Biomass Bioenerg. 122 (2019) 175-182.

[47] A. Gallifuoco, L. Taglieri, F. Scimia, A.A. Papa, G. Di Giacomo, New insights into the evolution of solid and liquid phases during hydrothermal carbonization of lignocellulosic biomasses, Biomass Bioenerg. 121 (2019) 122-127.

[48] J. Mumme, L. Eckervogt, J. Pielert, M. Diakite, F. Rupp, J. Kern, Hydrothermal carbonization of anaerobically digested maize silage, Bioresour. Technol. 102 (2011) 9255-9260.

[49] Y. Zhai, C. Peng, B. Xu, T. Wang, C. Li, G. Zeng, Y. Zhu, Hydrothermal carbonisation of sewage sludge for char production with different waste biomass: Effects of reaction temperature and energy recycling, Energy 127 (2017) 167-174.

[50] C. Rodriguez Correa, M. Bernardo, R.P.P.L. Ribeiro, I.A.A.C. Esteves, A. Kruse, Evaluation of hydrothermal carbonization as a preliminary step for the production of functional materials from biogas digestate, J. Anal. Appl. Pyrolysis 124 (2017) 461-474.

[51] V. Knappe, S. Paczkowski, J. Tejada, L.A. Diaz Robles, A. Gonzales, S. Pelz, Low temperature microwave assisted hydrothermal carbonization (MAHC) reduces combustion emission precursors in short rotation coppice willow wood, J. Anal. Appl. Pyrolysis 134 (2018) 162-166.

[52] A.V. Akkaya, Predicting Coal Heating Values Using Proximate Analysis via a Neural Network Approach, Energy Sources Part A-Recovery Util. Environ. Eff. 35 (2013) 253-260.

[53] D. Wang, F. Shen, G. Yang, Y. Zhang, S. Deng, J. Zhang, Y. Zeng, T. Luo, Z. Mei, Can hydrothermal pretreatment improve anaerobic digestion for biogas from lignocellulosic biomass?, Bioresour. Technol. 249 (2018) 117-124.

[54] N.B. Sebastien Michauda, Pierre Buffiere, Michel Roustan, Rene Moletta, Methane yield as a monitoring parameter for the start-up of anaerobic fixed film reactors, Water Res. 36 (2002) 1385-1391.

[55] E.S. Heidrich, T.P. Curtis, J. Dolfing, Determination of the internal chemical energy of wastewater, Environ. Sci. Technol. 45 (2011) 827-832.

[56] M. Heidari, S. Salaudeen, A. Dutta, B. Acharya, Effects of Process Water Recycling and Particle Sizes on Hydrothermal Carbonization of Biomass, Energy & Fuels 32 (2018) 11576-11586.

[57] S.T. Neeli, H. Ramsurn, Synthesis and formation mechanism of iron nanoparticles in graphitized carbon matrices using biochar from biomass model compounds as a support, Carbon 134 (2018) 480-490.

[58] O. Das, A.K. Sarmah, Z. Zujovic, D. Bhattacharyya, Characterisation of waste derived biochar added biocomposites: chemical and thermal modifications, Sci. Total Environ. 550 (2016) 133-142.

[59] C.Y. Hung, W.T. Tsai, J.W. Chen, Y.Q. Lin, Y.M. Chang, Characterization of biochar prepared from biogas digestate, Waste Manage. (Oxford) 66 (2017) 53-60.

[60] K.H. Kim, J.Y. Kim, T.S. Cho, J.W. Choi, Influence of pyrolysis temperature on physicochemical properties of biochar obtained from the fast pyrolysis of pitch pine (Pinus rigida), Bioresour. Technol. 118 (2012) 158-162.

[61] S. Ruile, S. Schmitz, M. Monch-Tegeder, H. Oechsner, Degradation efficiency of agricultural biogas plants--a full-scale study, Bioresour. Technol. 178 (2015) 341-349.

[62] Directive (EU) 2018/2001 of the European Parliament and of the Council of 11 December 2018 on the promotion of the use of energy from renewable sources, 2018.

[63] C. Sambusiti, F. Monlau, E. Ficara, A. Musatti, M. Rollini, A. Barakat, F. Malpei, Comparison of various post-treatments for recovering methane from agricultural digestate, Fuel Process. Technol. 137 (2015) 359-365.

[64] S. Menardo, P. Balsari, E. Dinuccio, F. Gioelli, Thermal pre-treatment of solid fraction from mechanically-separated raw and digested slurry to increase methane yield, Bioresour. Technol. 102 (2011) 2026-2032.

[65] H.B. Sharma, S. Panigrahi, A.K. Sarmah, B.K. Dubey, Downstream augmentation of hydrothermal carbonization with anaerobic digestion for integrated biogas and hydrochar production from the organic fraction of municipal solid waste: A circular economy concept, Sci. Total Environ. 706 (2020) 135907.

[66] Y. Yu, Z. Lei, X. Yang, X. Yang, W. Huang, K. Shimizu, Z. Zhang, Hydrothermal carbonization of anaerobic granular sludge: Effect of process temperature on nutrients availability and energy gain from produced hydrochar, Appl. Energy 229 (2018) 88-95.

[67] H.S. Kambo, A. Dutta, A comparative review of biochar and hydrochar in terms of production, physico-chemical properties and applications, Renew. Sustain. Energy. Rev. 45 (2015) 359-378.

[68] R.-Z. Wang, D.-L. Huang, Y.-G. Liu, C. Zhang, C. Lai, X. Wang, G.-M. Zeng, X.-M. Gong, A. Duan, Q. Zhang, P. Xu, Recent advances in biochar-based catalysts: Properties, applications and mechanisms for pollution remediation, Chem. Eng. J. 371 (2019) 380-403.

[69] X. Zhang, J. Xia, J. Pu, C. Cai, G.W. Tyson, Z. Yuan, S. Hu, Biochar-Mediated Anaerobic Oxidation of Methane, Environ. Sci. Technol. (2019).

[70] E.A.S.A. Council, Negative emission technologies: What role in meeting Paris Agreement targets?, EASAC policy report 35Available on https://easac.eu/publications/details/easac-net/, 2018.

[71] P. Smith, Soil carbon sequestration and biochar as negative emission technologies, Global change biology 22 (2016) 1315-1324.

[72] U. Ekpo, A.B. Ross, M.A. Camargo-Valero, P.T. Williams, A comparison of product yields and inorganic content in process streams following thermal hydrolysis and hydrothermal processing of microalgae, manure and digestate, Bioresour. Technol. 200 (2016) 951-960.
[73] D. Kim, K. Lee, K.Y. Park, Hydrothermal carbonization of anaerobically digested sludge for solid fuel production and energy recovery, Fuel 130 (2014) 120-125.
[74] Z. Cao, D. Jung, M.P. Olszewski, P.J. Arauzo, A. Kruse, Hydrothermal carbonization of biogas digestate: Effect of digestate origin and process conditions, Waste Manag. 100 (2019) 138-150.

List of Figures and Tables

Fig. 1. Hydrochar yield from: (1) untreated grass silage (UG), (2) digestate from untreated grass silage (DU), and (3) digestate from pre-treated grass silage (DP) under different temperatures.

Fig.2. Van-Krevelen diagram showing chemical changes in the feedstock and derived hydrochars.

Fig.3. Higher heating value (HHV) of the derived hydrochars.

Fig.4. Reducing sugar yield in the process liquor derived from the microwave assisted low-temperature hydrothermal treatment of: (a) untreated grass (UG), (b) digestate from untreated grass silage (DU), and (c) digestate from pre-treated grass silage (DP).

Fig.5. Soluble chemical oxygen demand (sCOD) in the process liquor derived from the microwave assisted low-temperature hydrothermal treatment of untreated grass silage (UG), digestate from untreated grass silage (DU), and digestate from pre-treated grass silage (DP).

Fig.6. Energy distribution in each product derived from the microwave assisted low-temperature hydrothermal treatment of: (a) untreated grass silage (UG), (b) digestate from untreated grass silage (DU), and (c) digestate from pre-treated grass silage (DP).

Fig.7. Carbon distribution during the entire processes of the two different scenarios: (a) AD + MLHT (at 180°C); (b) Acid pre-treatment (with 2% w/w sulphuric acid at 135°C for 15 minutes) + AD + MLHT (at 180°C).

Fig. 8. Scanning electron microscope (SEM) graphs of the substrates and corresponding hydrochars derived at 160 °C: (a) untreated grass silage (UG); (b) hydrochar derived from untreated grass silage (Char-UG-160); (c) digestate of untreated grass silage (DU); (d) hydrochar derived from digestate of untreated grass silage (Char-DU-160); (e) digestate of pre-treated grass silage (DP); (f) hydrochar derived from digestate of pre-treated grass silage (Char-DP-160).

Fig. 9. X-ray diffraction (XRD) patterns of the substrates and corresponding hydrochars derived at 160 °C, including for: untreated grass silage (UG), hydrochar derived from untreated grass silage (Char-UG-160), digestate of untreated grass silage (DU), hydrochar derived from digestate of untreated grass silage (Char-DU-160), digestate of pre-treated grass silage (DP), and hydrochar derived from digestate of pre-treated grass silage (Char-DP-160).

Fig. 10. Fourier transform infrared (FTIR) spectra of the substrates and corresponding hydrochars derived at 160 °C, including for: untreated grass silage (UG), hydrochar derived from untreated grass silage (Char-UG-160), digestate of untreated grass silage (DU), hydrochar derived from digestate of untreated grass silage (Char-DU-160), digestate of pre-treated grass silage (DP), and hydrochar derived from digestate of pre-treated grass silage (Char-DP-160).

Table 1 Compositional characteristics of the substrates for microwave assisted low-temperature hydrothermal treatment.

Table 2 Ash content and elemental compositions of the hydrochars derived at different temperatures

Table 3 Comparison of energy content of hydrochars obtained from different digestates in the literature.

Table 4 Comparison of net energy gain from anaerobic digestate with different post-treatments in the literature.

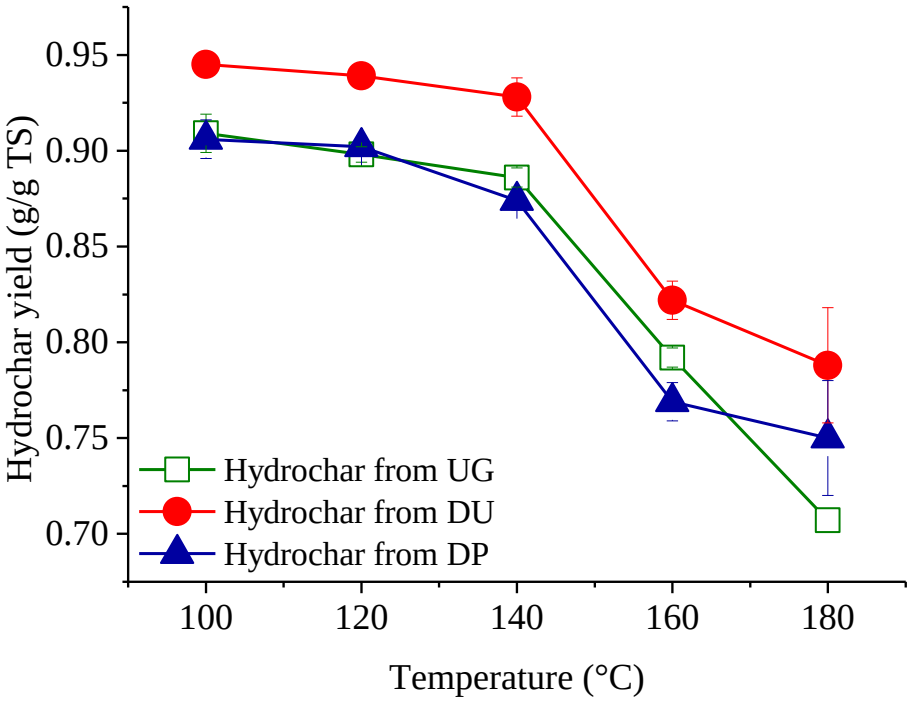


Fig. 1. Hydrochar yield from: (1) untreated grass silage (UG), (2) digestate from untreated grass silage (DU), and (3) digestate from pre-treated grass silage (DP) under different temperatures.

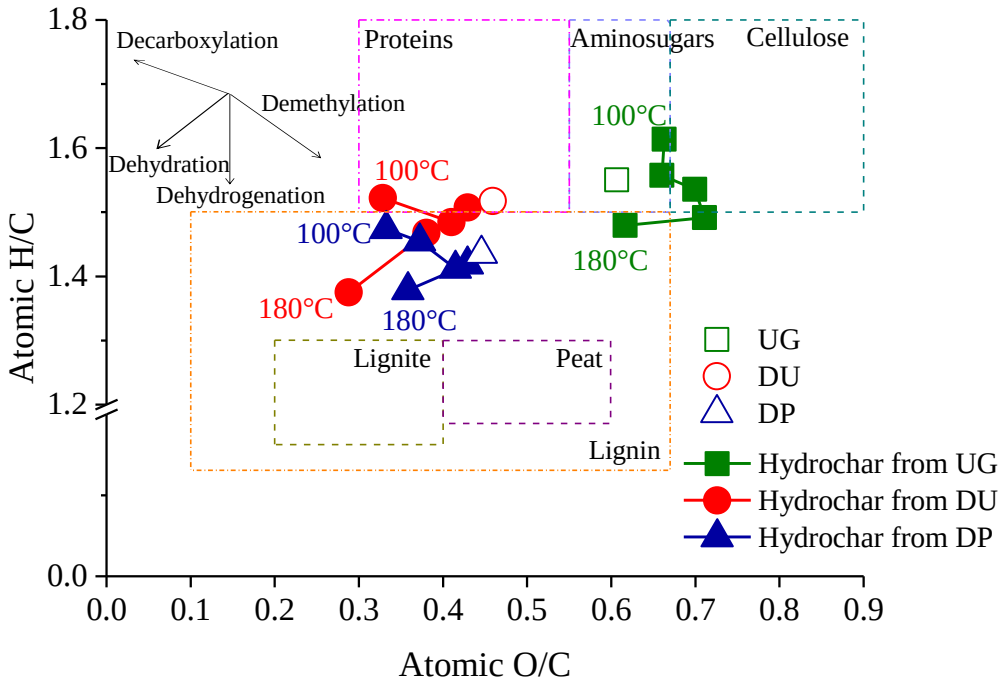


Fig.2. Van-Krevelen diagram showing chemical changes in the feedstock and derived hydrochars. UG: untreated grass silage, DU: digestate from untreated grass silage, and DP: digestate from pre-treated grass silage.

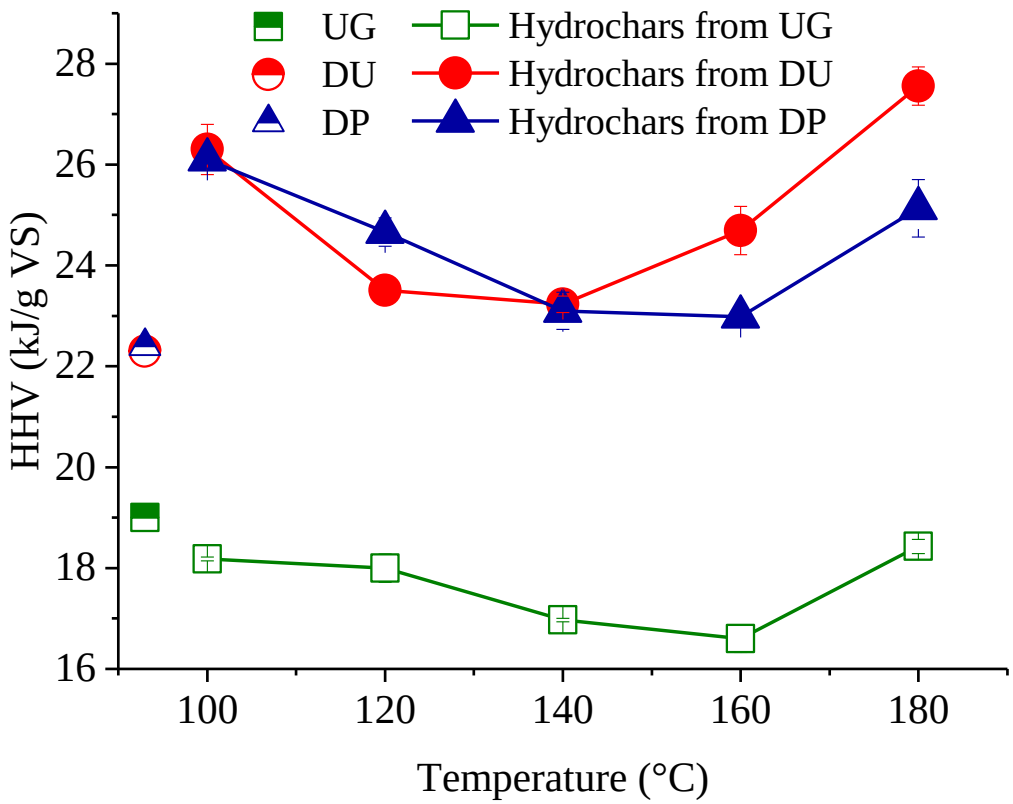


Fig.3. Higher heating value (HHV) of the derived hydrochars. UG: untreated grass silage, DU: digestate from untreated grass silage, and DP: digestate from pre-treated grass silage.

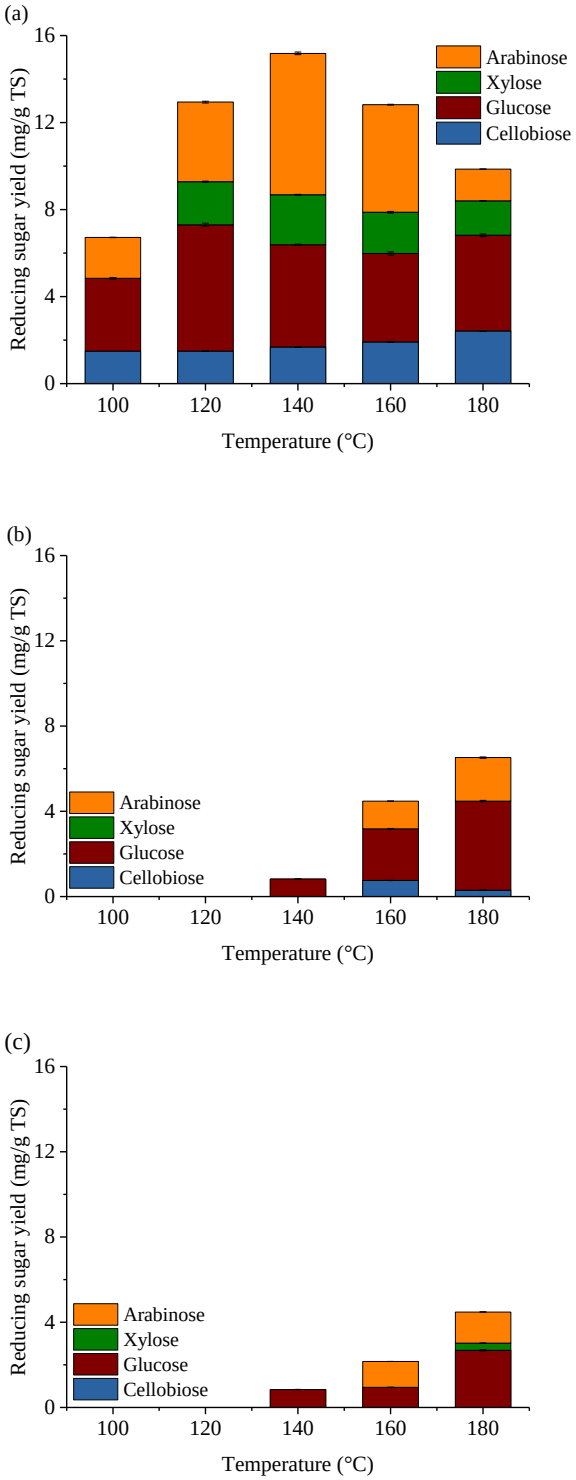


Fig.4. Reducing sugar yield in the process liquor derived from the microwave assisted low-temperature hydrothermal treatment of: (a) untreated grass (UG), (b) digestate from untreated grass silage (DU), and (c) digestate from pre-treated grass silage (DP).

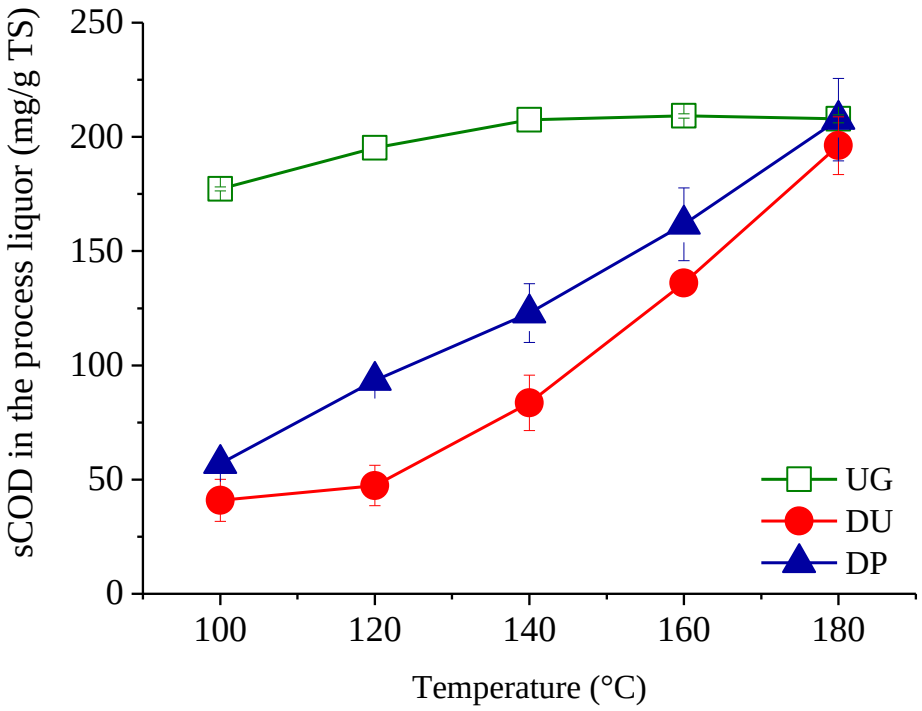


Fig.5. Soluble chemical oxygen demand (sCOD) in the process liquor derived from the microwave assisted low-temperature hydrothermal treatment of untreated grass silage (UG), digestate from untreated grass silage (DU), and digestate from pre-treated grass silage (DP).

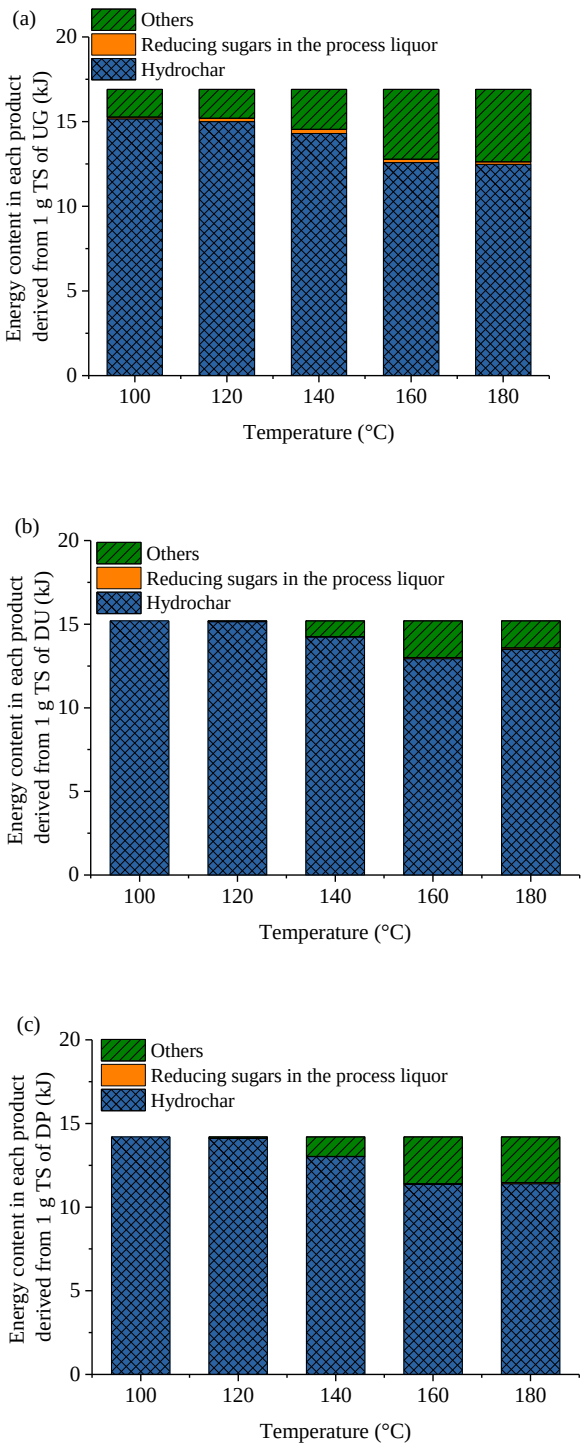


Fig.6. Energy distribution in each product derived from the microwave assisted low-temperature hydrothermal treatment of: (a) untreated grass silage (UG), (b) digestate from untreated grass silage (DU), and (c) digestate from pre-treated grass silage (DP).

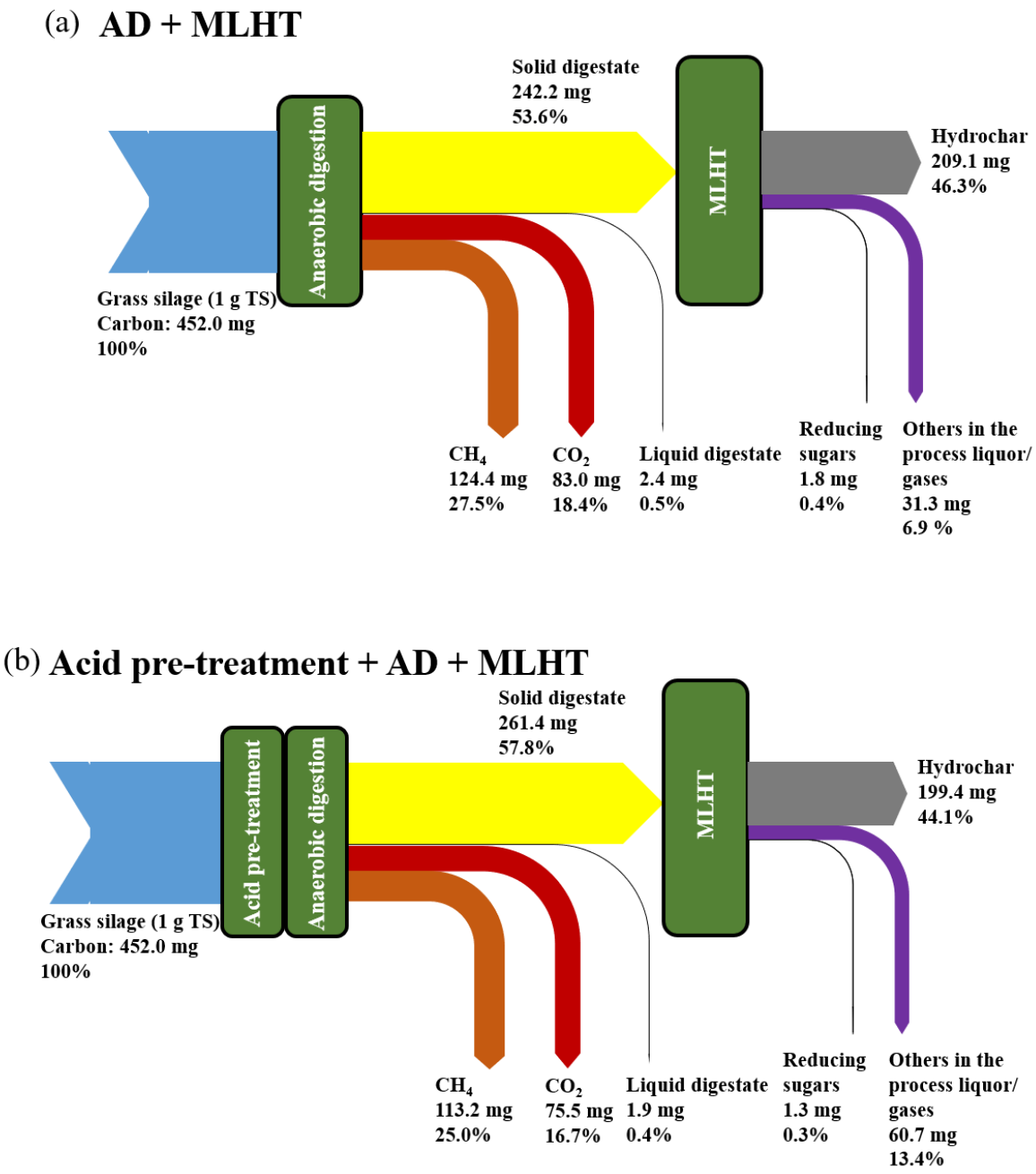


Fig.7. Carbon distribution during the entire processes of the two different scenarios: (a) AD + MLHT (at 180°C); (b) Acid pre-treatment (with 2% w/w sulphuric acid at 135°C for 15 minutes) + AD + MLHT (at 180°C). AD: anaerobic digestion, MLHT: microwave assisted low-temperature hydrothermal treatment.

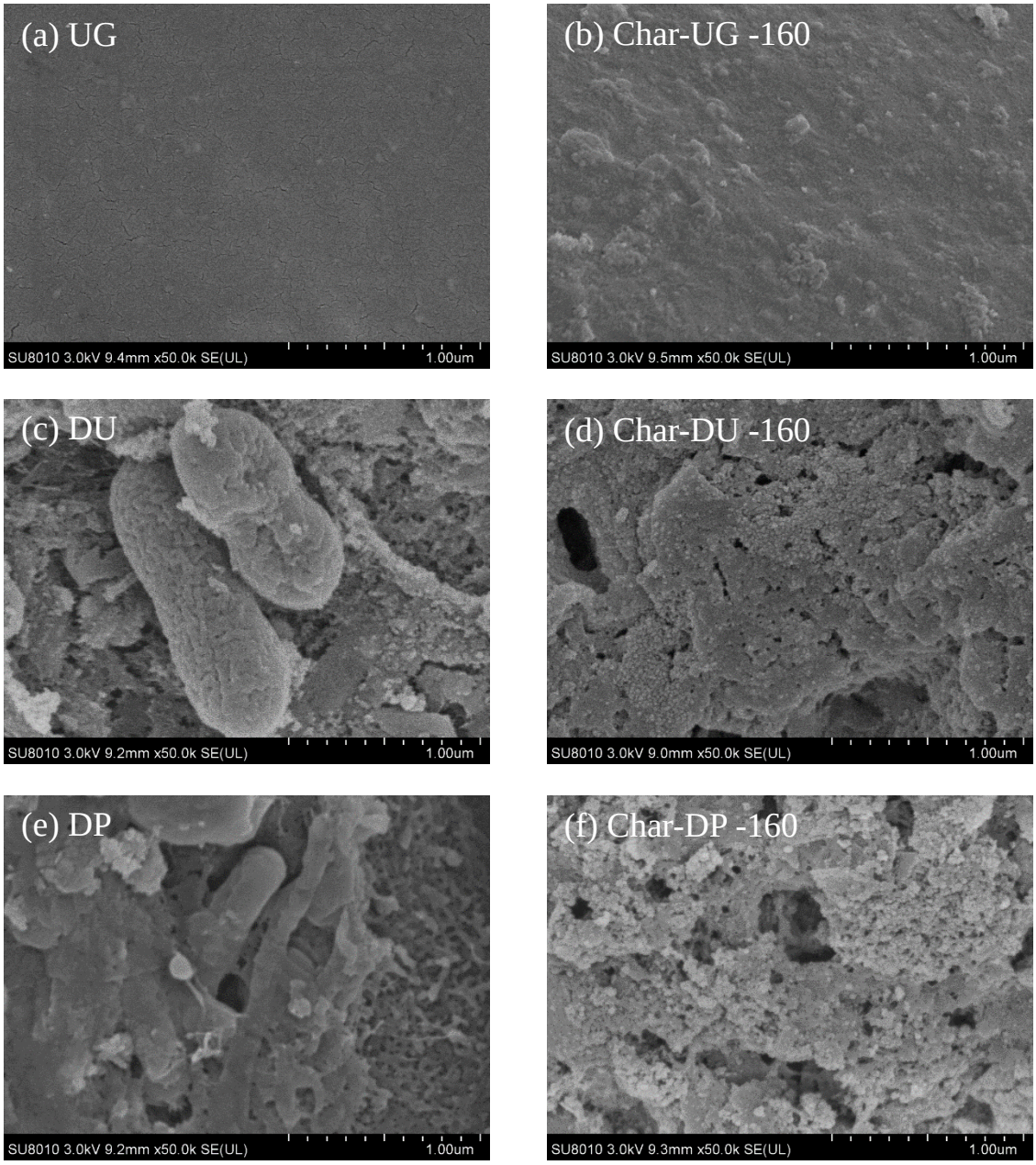


Fig. 8. Scanning electron microscope (SEM) graphs of the substrates and corresponding hydrochars derived at 160 °C: (a) untreated grass silage (UG); (b) hydrochar derived from untreated grass silage (Char-UG-160); (c) digestate of untreated grass silage (DU); (d) hydrochar derived from digestate of untreated grass silage (Char-DU-160); (e) digestate of pre-treated grass silage (DP); (f) hydrochar derived from digestate of pre-treated grass silage (Char-DP-160).

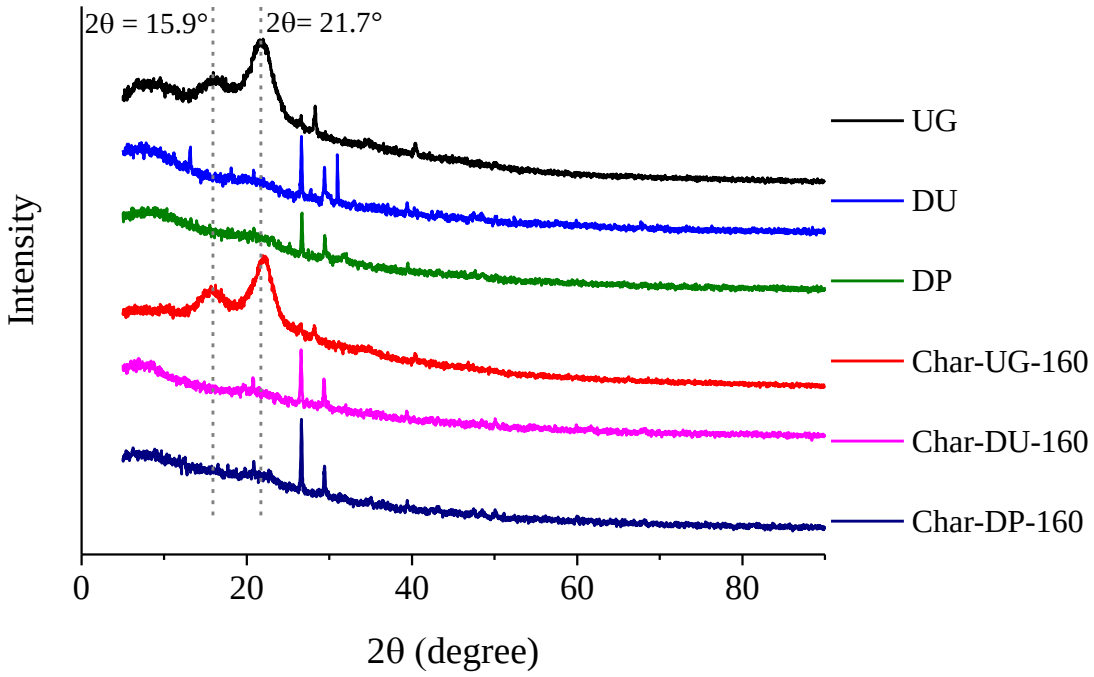


Fig. 9. X-ray diffraction (XRD) patterns of the substrates and corresponding hydrochars derived at 160 °C, including for: untreated grass silage (UG), hydrochar derived from untreated grass silage (Char-UG-160), digestate of untreated grass silage (DU), hydrochar derived from digestate of untreated grass silage (Char-DU-160), digestate of pre-treated grass silage (DP), and hydrochar derived from digestate of pre-treated grass silage (Char-DP-160).

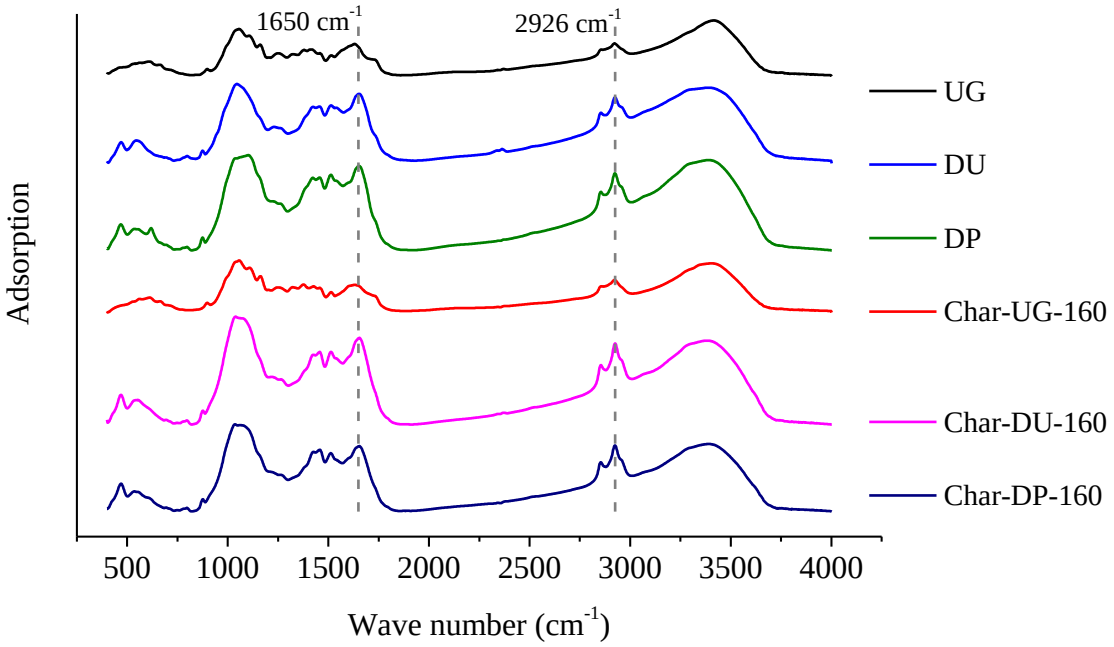


Fig. 10. Fourier transform infrared (FTIR) spectra of the substrates and corresponding hydrochars derived at 160 °C, including for: untreated grass silage (UG), hydrochar derived from untreated grass silage (Char-UG-160), digestate of untreated grass silage (DU), hydrochar derived from digestate of untreated grass silage (Char-DU-160), digestate of pre-treated grass silage (DP), and hydrochar derived from digestate of pre-treated grass silage (Char-DP-160).

Table 1 Compositional characteristics of the substrates for microwave assisted low-temperature hydrothermal treatment.

	Untreated grass silage (UG)	Solid digestate from untreated grass silage (DU)	Solid digestate from pretreated grass silage (DP)
Proximate analysis (wt %)			
VS/TS	89.1±1.0	68.3±2.1	64.7±1.3
Ash/TS	10.9±0.1	31.7±2.0	35.3±1.3
Elemental analysis (% VS)			
Carbon	50.5±0.2	54.4±0.2	55.5±1.3
Hydrogen	6.5±0.0	6.9±0.0	6.6±0.1
Oxygen	41.3±0.1	33.3±0.2	33.0±1.5
Nitrogen	1.7±0.2	5.4±0.1	4.9±0.0
Energy value (kJ/g TS)	16.9	15.2	14.5
Energy value (kJ/g VS)	19.0	22.3	22.4

Table 2 Ash content and elemental compositions of the hydrochars derived at different temperatures

Hydrochar name	Feedstock	Temperature (°C)	Ash (% TS)	Elemental analysis (% VS)			
				C	H	N	O
Char-UG-100	Untreated grass silage	100	8.3±0.3	48.9±0.1	6.6±0.0	1.3±0.1	43.3±0.0
Char-UG-120	Untreated grass silage	120	7.2±1.2	49.2±0.3	6.4±0.1	1.0±0.1	43.4±0.3
Char-UG-140	Untreated grass silage	140	4.9±1.4	48.0±0.1	6.1±0.0	1.1±0.1	44.8±0.0
Char-UG-160	Untreated grass silage	160	3.9±0.2	47.8±0.4	6.0±0.0	0.9±0.1	45.3±0.4
Char-UG-180	Untreated grass silage	180	4.2±0.2	50.2±0.3	6.2±0.0	2.4±0.2	41.2±0.1
Char-DU-100	Digestate of untreated grass silage	100	33.0±1.1	59.5±0.6	7.5±0.1	6.9±0.4	26.1±1.0
Char-DU-120	Digestate of untreated grass silage	120	31.4±0.0	56.2±0.0	7.0±0.1	6.1±0.2	30.8±0.1
Char-DU-140	Digestate of untreated grass silage	140	33.9±0.8	55.9±0.3	7.0±0.0	5.1±0.1	32.0±0.3
Char-DU-160	Digestate of untreated grass silage	160	36.3±0.3	58.5±0.3	7.1±0.1	4.7±0.5	29.7±1.0
Char-DU-180	Digestate of untreated grass silage	180	37.9±0.0	63.6±0.5	7.3±0.1	4.6±0.0	24.5±0.6
Char-DP-100	Digestate of pre-treated grass silage	100	34.4±1.0	60.0±0.1	7.4±0.1	5.9±0.1	26.6±0.3
Char-DP-120	Digestate of pre-treated grass silage	120	35.7±1.1	58.3±0.4	7.1±0.1	5.8±0.0	28.9±0.4
Char-DP-140	Digestate of pre-treated grass silage	140	35.6±0.2	56.6±0.1	6.7±0.3	5.5±0.0	31.3±0.2
Char-DP-160	Digestate of pre-treated grass silage	160	35.0±0.8	56.7±0.1	6.7±0.0	4.1±0.1	32.5±0.3
Char-DP-180	Digestate of pre-treated grass silage	180	39.4±0.1	60.3±0.5	6.9±0.2	4.0±0.1	28.8±0.8

UG: untreated grass silage, DU: digestate from untreated grass silage, and DP: digestate from pre-treated grass silage.

Table 3 Comparison of energy content of hydrochars obtained from different digestates in the literature.

Feedstock	HHV of feedstock (kJ/g, dry basis)	Process	Process temperature (°C)	Time (min)	HHV of hydrochar (kJ/g, dry basis)	Energy densification	Ref
Solid digestate from untreated grass silage	22.3 (ash-free)	MLHT	180	30	27.6 (ash-free)	1.24	This study
Solid digestate from pre-treated grass silage	22.4 (ash-free)	MLHT	180	30	25.1 (ash-free)	1.12	This study
Digested sewage sludge	7.8	HTC	170	60	5.5	0.71	[72]
			250	60	4.3	0.55	
Digested sludge	16.5	HTC	180	30	17.3	1.05	[73]
			200	30	17.5	1.06	
			220	30	18.3	1.11	
Digested sewage sludge	16.5	HTC	150	60	17.3	1.05	[45]
			180	60	17.5	1.06	
Digested maize silage	22.3 (ash-free)	HTC	190	120	25.4 (ash-free)	1.14	[48]
			230	120	30.3 (ash-free)	1.36	
Digestate from maize and grass silage	17.8	HTC	150	60	17.9	1.01	[40]
			200	60	20.7	1.16	
Digested sewage sludge	14.9	HTC	150	60	15.0	1.01	[40]
			200	60	15.1	1.01	
Digestate from household waste containing vegetable, garden, and fruit	14.9	HTC	150	60	15.0	1.01	[40]
			200	60	15.1	1.01	
Digestate from mixture of cow manure, maize silage, grass silage, and cereals	16.4	HTC	170	120	15.5	0.95	[74]
			190	120	15.7	0.96	
Digestate from cow manure and cow dung	17.0	HTC	170	120	17.1	1.01	[74]
			190	120	17.6	1.04	
Digestate from yard waste	15.6	HTC	180	360	20.5	1.31	[65]
			200	360	21.5	1.37	

MLHT: microwave assisted low-temperature hydrothermal treatment; HTC: conventional hydrothermal carbonation.

Table 4 Comparison of net energy gain from anaerobic digestate with different post-treatments in the literature.

Digestate feedstock	Process	Process parameters	Methane potential before treatment (ml/g TS in digestate)	Methane potential post treatment (ml/g TS in digestate)	Hydrochar yield (ml/g TS in digestate)	Increment in methane potential (ml/g TS in digestate)	Increment of energy in methane (kJ/g TS in digestate)	Energy in hydrochar (kJ/g TS in digestate)	Energy required for process operation (kJ/g TS in digestate)	Net energy gain (kJ/g TS in digestate)	Ref
DU	MLHT	180 °C, 30 min,4.7% solid	< 7.0 (process liquor)	68.7 (process liquor)	0.79	881%	2.5	13.5	13.6	2.3	This study
DP	MLHT	180 °C, 30 min, 4.7% solid	< 7.0 (process liquor)	72.7 (process liquor)	0.75	939%	2.6	11.4	13.6	0.4	This study
Digested sludge	HTC	130°C (0.1 MPa), 30 min, 1.4% solid	47.0 (mixture)	161.0 (mixture)	/	243%	4.5	/	31.3	-26.8	[14]
		170 °C (0.1 MPa), 30 min, 1.4% solid	47.0 (mixture)	166.1 (mixture)	/	253%	4.7	/	43.3	-38.6	
		210 °C (0.1 MPa), 30 min, 1.4% solid	47.0 (mixture)	130.1 (mixture)	/	177%	3.3	/	55.2	-51.9	
Digested sewage sludge	HTC	220 °C (3.5 MPa), 30 min, 4.5% solid	7.2 (process liquor)	80.0 (process liquor)	0.74	1011%	2.9	10.5	18.1	-4.7	[16]
		160 °C (0.5 MPa), 30 min, 4.5% solid	7.2 (process liquor)	75.8 (process liquor)	0.69	953%	2.7	11.7	12.5	1.9	
Digested microalgae	HTC	200 °C (0.1 MPa), 0 min, 1.25% solid	63.9 (mixture)	153.9 (mixture)	/	141%	3.6	/	58.5	-54.9	[15]
Solid digestate from Napier grass	HTC	240 °C (0.3 MPa), 60 min, 14.3% solid	/	/	0.45	/	/	11.5	6.3	5.2	[12]

DU: digestate from untreated grass silage; DP: digestate from pre-treated grass silage; MLHT: microwave assisted low-temperature hydrothermal treatment; and HTC: conventional hydrothermal carbonation.

***Declaration of Interest Statement**

Declaration of interests

☒ The authors declare that they have no known competing financial interests or personal relationships that could have appeared to influence the work reported in this paper.

☐The authors declare the following financial interests/personal relationships which may be considered as potential competing interests: